JOURNAL OF CATALYSIS **158,** 205–216 (1996)
ARTICLE NO. 0020

Oxide Supported MoS_2 Catalysts of Unusual Morphology

A. K. Datye,*,[1] S. Srinivasan,*,[2] L. F. Allard,† C. H. F. Peden,‡ J. R. Brenner,§ and L. T. Thompson§

**Center for Microengineered Ceramics and Department of Chemical & Nuclear Engineering, University of New Mexico, Alburqerque, New Mexico 87131; †High Temperature Materials Laboratory, Oak Ridge National Laboratory, Oak Ridge, Tennessee 37831; ‡Molecular Sciences Research Center, Pacific Northwest Laboratories, Richland, Washington 99352; and §Department of Chemical Engineering, University of Michigan, Ann Arbor, Michigan 48109*

Received January 17, 1995; revised September 6, 1995; accepted September 11, 1995

Two different titanias were used as supports for MoS_2 catalysts, Degussa P25 titania and a microroughened titania prepared in our laboratory. The Mo weight loading was varied to study the effect of loading on the pyridine hydrodenitrogenation activity. It was found that the specific activity of sulfided molybdena on the P25 titania decreased monotonically with increasing loading. On the other hand, the microroughened titania did not show such a fall off in activity; furthermore its specific activity was over an order of magnitude greater than that of the P25-supported sample. The rather surprising behavior of MoS_2 supported on microroughened titania can be related to the structure of the catalyst. On the microroughened titania, the MoS_2 sheets are curved with radii of curvature ranging from 2–5 nm. These strained MoS_2 layers could lead to the formation of unique catalytically active sites in the basal plane of MoS_2, not otherwise obtained on conventional supports.

INTRODUCTION

Hydrotreating is an important catalytic process that consumes significant amounts of catalyst each year (1). Stricter environmental standards also necessitate a push toward more active catalysts. Consequently, the roles of the support and promoters are being actively investigated. Recent reports in the literature suggest that titania supports may yield hydrodesulfurization catalysts that are four times more active than conventional alumina supported catalysts (2–4). However, the low surface areas, poor thermal stabilities of the anatase phase, poor abrasion resistance, and difficulties in extruding titania make these supports less desirable. In this study, we have synthesized a novel, "microengineered" form of titania that overcomes some of limitations of catalysts based on bulk titania. We present the characterization and reactivity of hydrotreating catalysts consisting of MoS_2 supported on this microengineered TiO_2.

Molybdenum sulfide catalysts are amenable to examination using the transmission electron microscope since the interplanar spacing of the basal planes of MoS_2 is large enough to be easily resolved. In the literature, two kinds of morphologies have been proposed for MoS_2 on oxide supports: the "bookend" morphology and the "basal plane" morphology. Pratt *et al.* (5) suggested that the bookend morphology was stabilized on silica and alumina and the basal plane morphology on titania and zirconia. These differing morphologies would, according to them, explain the catalytic behavior of these catalysts with increasing molybdena loading. It is commonly accepted that the active sites in sulfided molybdena catalysts are located at the edge of the MoS_2 planes, with the coordinatively saturated Mo atoms in the basal plane being less reactive (6). On titania, increasing amounts of molybdena would result in larger domains of MoS_2, with the ratio of edge sites to total sites decreasing with domain size. On the other hand, no such decrease would be expected on alumina supports since increasing molybdena loading would only increase the number of bookends but not affect the ratio of edge to basal plane atoms.

Previous microscopy studies have used commercially available oxide supports which possess a tortuous three-dimensional pore structure that makes it difficult to deduce the morphology of the supported MoS_2. We have demonstrated that nonporous oxide supports of simple geometry facilitate TEM characterization of the catalytically active phase in heterogeneous catalysts (7). Therefore, to unambiguously identify the morphology of the supported MoS_2 (8), we used nonporous model supports consisting of microspheres of silica, titania, and alumina. We found that the basal plane morphology was the only one detected on all of the supports we studied. A similar conclusion was reached by Delannay (9) and Payen *et al.* (10) who found that the basal plane morphology was the only one they could unambiguously identify on supports such as γ-Al_2O_3

---

[1] To whom correspondence should be addressed.

[2] Present address: Department of Chemical Engineering, University of California, Berkeley, CA 94720.

0021-9517/96 $12.00

and $CoAl_2O_4$. Given that MoS_2 adopts a similar morphology on all supports, it is surprising that the observed effect of MoS_2 loading is so different for alumina and titania supports (5).

Our high resolution TEM images (8) suggested specific differences in the alumina and titania supports that could account for their catalytic behavior with increasing coverage. Silica and alumina are available as high surface area powders and they have considerably rougher surfaces than titania powders which are generally available in low surface area form. Alumina surfaces are inherently rough because they are formed by dehydration of boehmite, where the loss of water leaves behind voids in the oxide. On the other hand, P25 titania is prepared by flame hydrolysis at elevated temperatures which helps form individual single crystals of anatase and rutile phases, but with no internal porosity. These microscale surface textural differences would be expected to affect the nucleation and growth of MoS_2 crystallites on the oxide surface. The microscopically smooth surfaces of titania would provide fewer nucleation sites leading to larger domains of MoS_2 as the surface coverage of molybdena was increased. The larger MoS_2 domains would have fewer edge sites per deposited Mo, yielding lower specific activities with increasing coverage. On the other hand, the rougher alumina surfaces would provide a greater number of nucleation sites and the MoS_2 domains would have less chance to grow into large islands, maintaining the high ratio of edge to basal plane sites with increasing coverage of molybdena.

At low loadings, the titania-supported MoS_2 is at least four times more active than alumina-supported MoS_2 (5, 11), however as the loading is increased the catalyst activity drops below that of the alumina-supported catalyst (5). The high activity of MoS_2 supported on titania supports prompted us to prepare catalysts in which some of the detrimental features of bulk titania were avoided. Since molybdena is known to wet and spread on titania, but not on silica (12), we can control the size of MoS_2 domains by depositing nanometer-sized particles of titania on silica. On such a catalyst, even when the coverage corresponds to a monolayer of MoS_2 on titania, the limited size of the MoS_2 islands ensures that edge sites are still available. These model catalysts allow us to study the role of surface roughness and texture on the nature of active sites in hydrotreating catalysts. As we show in this paper, the reactivity results appear to confirm the hypothesis that a rougher surface texture prevents the fall off in activity with increasing surface coverage that is normally seen with fumed titania supports. In fact we observed that the activity of these microengineered catalysts far exceeded that of MoS_2 on bulk titania, an effect we believe is related to the radius of curvature of the MoS_2 slabs on these catalysts. The strained MoS_2 layers could lead to the formation of unique catalytically active sites in the basal planes of MoS_2, not otherwise obtained on conventional supports.

EXPERIMENTAL

Catalyst Preparation

Two supports were used in this study: fumed titania and titania/silica. The fumed titania (P25) was obtained from Degussa A. G. and is prepared by flame hydrolysis of the respective chloride. The titania/silica consisted of a monolayer coating of titania dispersed on microspheres of silica, 200 nm in diameter. The silica spheres were prepared by the procedure of Stöber *et al.* (13) and had a surface area of 15 m^2/g. Titania monolayer coatings were achieved by contacting the silica with a solution of titanium isopropoxide in THF under an N_2 atmosphere and washing off the excess alkoxide with THF. This procedure yields about 1.5 wt% titania on silica; further details have been reported elsewhere (14, 15). The molybdena was supported on these oxides by calcination of a physical mixture of an appropriate weight of MoO_3 and the respective support for a period of 3 hr at 773 K. Previous work has shown that this treatment causes the molybdena to spread on the titania (12).

Neutron Activation Analysis

Neutron activation analysis (NAA) was conducted in order to assess the elemental composition of the catalysts. The samples that were analyzed included a blank, a MoO_3 standard (99.95% metals basis, Alfa), three dried Mo atomic absorption (AA) standards (1000 #177# 10 ppm, Fisher Scientific), and three NIST-SRM-1663a standards for Ti. The characteristic γ-ray energies and half-lives used for this analysis were as follows: Mo (306.9 kV, 14.2 min; 140.5 kV, 66.02 hr), Ti (320.1 kV, 5.76 min). Silicon has a half-life which is too short to practically count.

The neutron activation analysis consisted of a short (P-tube) and long (in-core) irradiation with γ-ray spectroscopy after each irradiation. The first irradiation lasted 1 min. Following an 11 min decay, radiation from each sample was counted for 8 min to determine the Ti concentration and an approximate Mo concentration. The samples were then irradiated for 30 min in-core, and the radiation was counted for 2 days. This information was used to estimate the Mo content. The resulting concentrations have been reported as MoO_3 and TiO_2, respectively.

Oxygen Chemisorption

Oxygen chemisorption was used to estimate the site density. Because oxygen can dissolve into the sulfide lattice (16), we used the dynamic pulsed adsorption technique at low temperatures to distinguish bulk adsorption from

TABLE 1

Elemental Analysis by Neutron Activation of the Catalysts Used in This Study

Sample	Ti as TiO_2 Nominal (%)	Ti as TiO_2 Experimental (%)	Ti as TiO_2 St. dev. (%)	Mo loading as MoO_3 Nominal (%)	Mo loading as MoO_3 Experimental (%)	Mo loading as MoO_3 St. dev. (%)
0.5 wt% Mo/TiO_2/SiO_2		2.5	0.2	0.5	0.54	0.06
1.0 wt% Mo/TiO_2/SiO_2		2.7	0.2	1.0	1.3	0.1
2.0 wt% Mo/TiO_2/SiO_2		2.8	0.2	2.0	2.3	0.1
2.0 wt% Mo/TiO_2	98.0	97.0	4.9	2.0	2.6	0.2
4.0 wt% Mo/TiO_2	96.0	94.0	4.8	4.0	4.4	0.3
6.0 wt% Mo/TiO_2	94.0	100.1	4.7	6.0	4.7	0.3
8.0 wt% Mo/TiO_2	92.0	93.2	4.4	8.0	6.4	0.4
10.0 wt% Mo/TiO_2	90.0	90.5	4.2	10.0	10.4	0.6

uptake at MoS_2 edge sites (17). Oxygen uptake experiments were carried out using a Quantasorb sorption analyzer. The pretreatment protocol consisted of purging the catalyst bed with He, followed by reduction in H_2 at 673 K for at least 4 hr. The catalyst was purged with He before it was cooled to room temperature. The sorption experiments consisted of submerging the sample loop containing the catalyst into a dry ice/acetone bath (195 K), followed by O_2 adsorption from a 9.98% O_2/He mixture until the surface was saturated.

Transmission Electron Microscopy

The sample preparation for the transmission electron microscopy involved supporting the powder on a 3-mm. Cu TEM grid covered by a holey carbon film. Observations were performed on a JEOL 4000 EX operated at 400 keV and a JEOL 2000 FX operated at 200 keV. Some of the images were also obtained on a Hitachi HF 2000 field emission TEM.

Pyridine HDN Activity Measurements

Approximately 0.5 g of catalyst was loaded into a Pyrex flow reactor over a plug of glass wool. A thermocouple was placed directly into the catalyst bed, and the catalyst temperature was held to within ±1 K of the set point. Prepurified He and H_2 were further purified during passage through a commercial combination oxygen and moisture trap (Matheson). The catalysts were purged in He at room temperature, pyrolyzed by heating in He up to 673 K, and then sulfided for 5 hr in a 2% H_2S/H_2 mixture at 673 K. Prior to the reaction rate measurements, the catalysts were reduced overnight at 673 K in flowing H_2.

The reactants and products were separated using a 1.8 m Hayesep D column (Alltech) and analyzed using a Hewlett Packard 5890 gas chromatograph. Peak areas and retention times were determined using a SpectraPhysics integrator and calibrated using standard alkane and alkene gas mixtures (Scott, #177# 2%). Activities were measured under differential conditions (conversion $< 5\%$) at 633–673 K and atmospheric pressure using a reactant mixture containing 0.6% pyridine (Aldrich, 99+%) in H_2. The catalytic properties went through an initial transient of greater than 15 min but not more than 1 hr. Negligible deactivation occurred after holding the reaction temperature at 673 K for 4 hr. The temperature was held at 673 K for 3 hr, 648 K for 2 hr, and then 633 K for 2 hr. The conversion multiplied by the flow rate did not change when the flow rate was varied between 5 and 20 sccm., confirming the absence of external mass transport limitations.

RESULTS

Table 1 lists the results of the elemental analysis of all of the catalysts used in this study. The nominal weight loading is quite close to the loading determined by NAA. The surface loading of the MoS_2/TiO_2 catalysts ranges from 2.1 to 8.7 Mo/nm^2 which is similar to those used in earlier studies; for example, Pratt *et al.* (5) covered a range from 0.97 to 9.73 Mo/nm^2. The monolayer loading of MoS_2 based on its basal plane surface area of $\approx$8.5 Å^2 (18) corresponds to 11.6 Mo/nm^2. Therefore, these catalysts have loadings corresponding to less than that of a monolayer of MoS_2.

Figures 1–4 show TEM images of the MoS_2/TiO_2 catalysts. Figure 1 shows an image of the 2.3 wt% catalyst obtained after the catalyst was sulfided in 10% H_2S at 773 K. The sample was exposed to air after removal from the reactor before being examined in the TEM. This image shows that most of the titania surface is bare and only isolated regions exhibit the single dark lines that correspond to single layer MoS_2 sheets on the titania surface. These black lines are indicated by arrows in this figure. Multilayers of MoS_2 are not seen on this sample which is

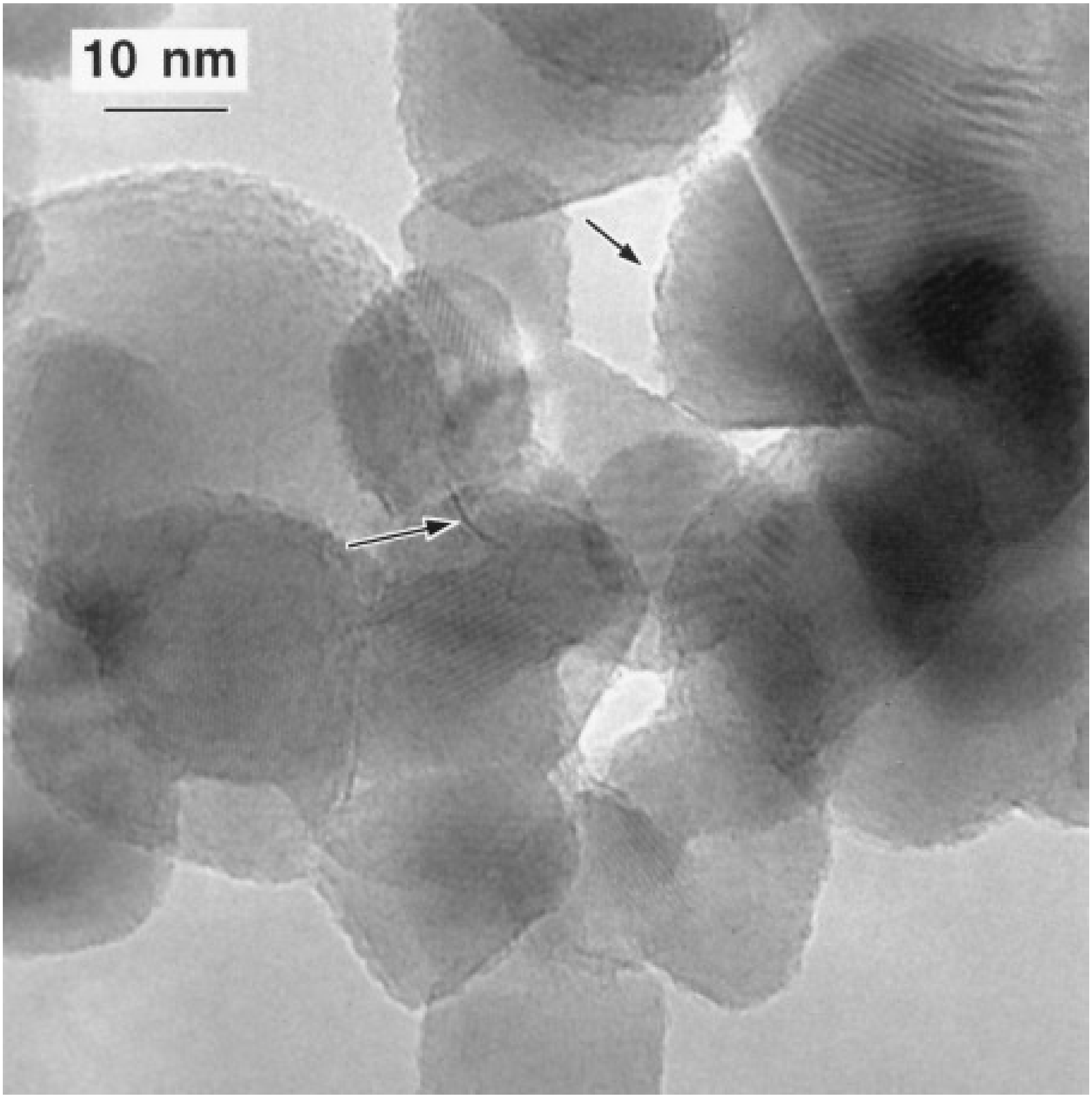

FIG. 1. Micrograph of 2.3 wt% MoO_3 Degussa P25 TiO_2 after the catalyst was sulfided in 10% H_2S/H_2 at 773 K. The surface of TiO_2 is bare with isolated dark lines that indicate the presence of single layers of MoS_2 (arrowed).

consistent with the low loading of 2.1 Mo/nm^2 compared to 11.6 Mo/nm^2 required for monolayer coverage. Figures 2 and 3 show images of the 4.7 and 10.4 wt% MoO_3/TiO_2 catalyst after sulfidation and use in the HDN reaction. We find that the surface coverage by the MoS_2 is much greater in these samples. The majority of the sample seems to be covered by black lines that indicate the presence of single layers of MoS_2, however, isolated instances of multilayers of MoS_2 are seen. The oxygen chemisorption of these samples does increase with increasing loading but not linearly with loading. We assume that oxygen titrates only the edge sites of MoS_2. If we also assume that it is the size rather than the number of MoS_2 islands that increases with increasing loading, then the number of edge sites will vary linearly with the diameter (d) of these islands, whereas the loading would be proportional to the area which varies as d^2. This would imply a square root relationship between chemisorption and loading, which is approximately obeyed by this sample.

Figures 4–6 show the morphology of MoS_2 on the titania-coated silica support. Addition of MoO_3 to a titania/silica sample leads to an increase in the surface roughness as we described previously (8). On these samples, the titania is present as nanometer-sized protuberances resulting in

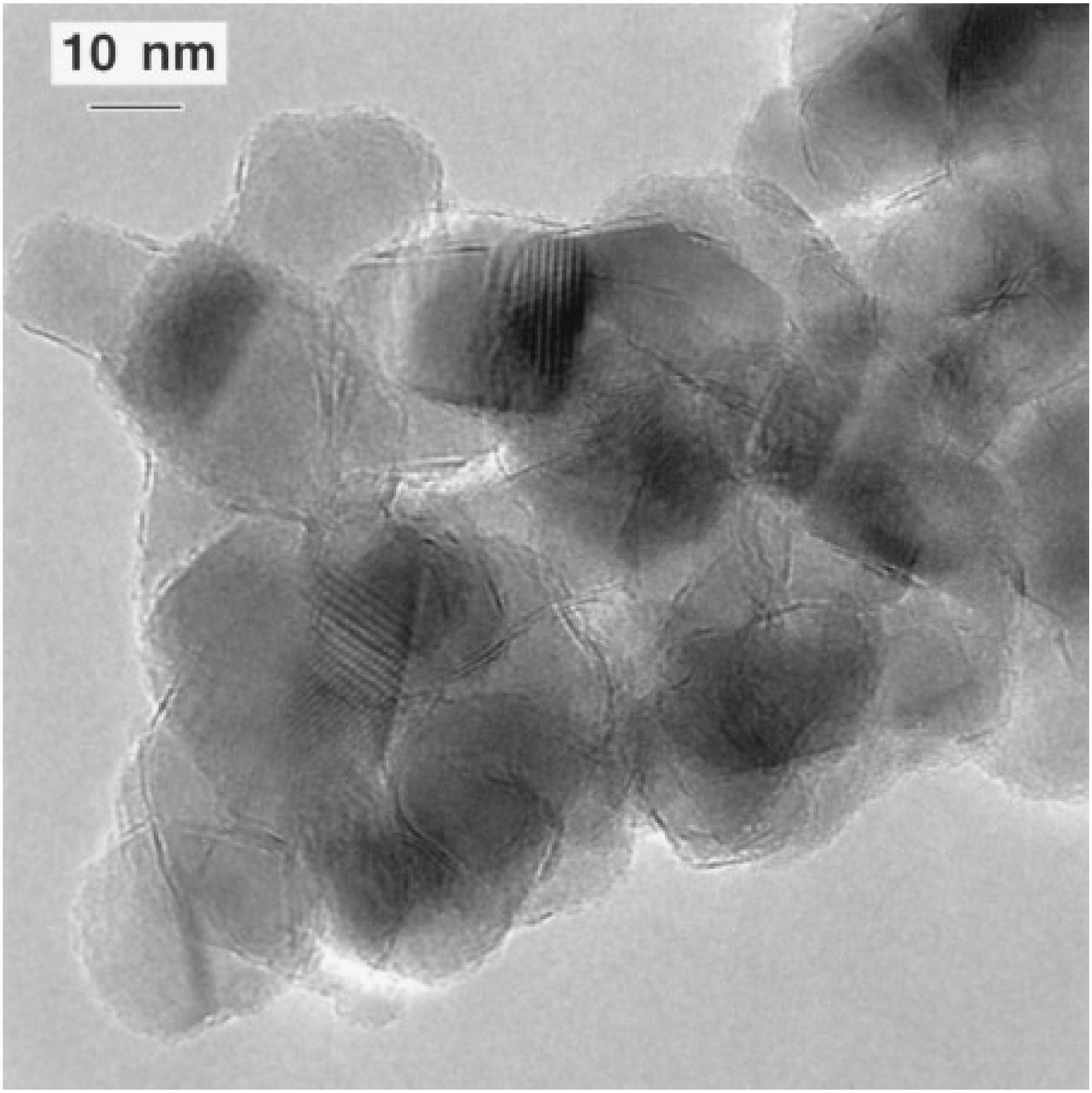

FIG. 2. Micrograph of 4.7 wt% MoO_3 Degussa P25 TiO_2 after the catalyst was sulfided in 10% H_2S/H_2 at 773 K. A greater coverage of the TiO_2 by MoS_2 is evident.

what could be described as a microroughened surface. The titania-coated silica was prepared in a single batch of 11 g, portions of which were used to add varying amounts of MoO_3. All these samples contain approximately 2.5 wt% TiO_2 on 200-nm silica spheres. Figure 4a shows a low magnification view of the sample which contains 0.54 wt% MoO_3 supported on the titania/silica after sulfiding and use in the HDN reaction. Consistent with the loading of MoS_2, dark lines are few and far between on this sample indicating that the coverage is considerably below that of a monolayer of MoS_2. If we assume that the surface area of the titania is equal to that of the silica spheres (15 m^2/g), the Mo loading would be 1.5 Mo/nm^2, compared with 11.6 Mo/nm^2 for a monolayer. Since the titania forms hemispherical protuberances on the surface, their exposed surface area would be different. As an approximation, if we use the equations $S = 6/\rho d$ where ρ is 4.25 g/cm^3 for anatase TiO_2 and the diameter of the protuberances is 5 nm, we can estimate the TiO_2 surface area to be 7 m^2/g for a 2.5 wt% TiO_2 loading on the silica. Therefore, the surface coverage of the 0.54 wt% sample is closer to 3.2 Mo/nm^2. A higher magnification view of this sample, Fig. 4b, shows well-resolved crystallites of TiO_2 on the silica, but no trace of the dark lines that indicate the presence of MoS_2, consistent with the low surface coverage.

The titania surfaces (arrowed in Fig. 4) in the 0.54 wt%

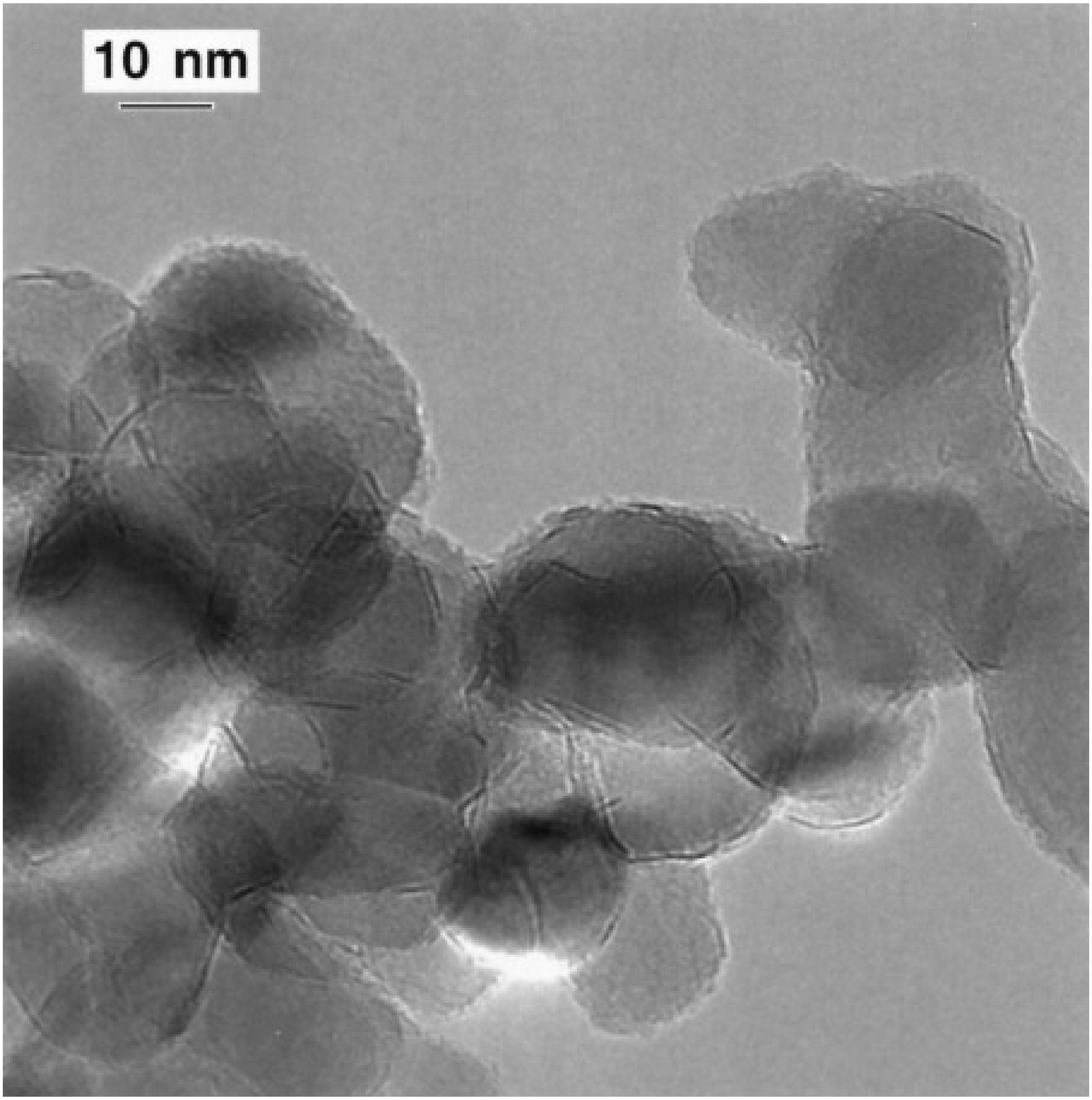

FIG. 3. Micrograph of 10.4 wt% MoO_3 Degussa P25 TiO_2 after the catalyst was sulfided in 10% H_2S/H_2 at 773 K. Most of the MoS_2 is in the form of single dark lines but some instances of multilayers of MoS_2 are visible (arrowed).

catalyst can be contrasted with those on the higher loaded samples (Figs. 5 and 6). The catalyst that contained 1.3 wt% MoO_3 on TiO_2/SiO_2 (Fig. 5) is seen to have much of the titania surface covered with MoS_2. The loading of this sample corresponds to ~7.7 Mo/nm^2, a number that is about half a monolayer. There are two types of MoS_2 morphologies that are illustrated in this micrograph: flat sheets of MoS_2, which may form on the silica surface, and those that are curved and conform to the curvature of the underlying titania. The MoS_2 sheets on the silica are similar to those reported by us previously (8), and they appear flat due to the large radius of curvature of the silica (100 nm) compared to that of the titania (2–5 nm).

With increasing coverage of the MoS_2, we find that a larger fraction of the titania surface is covered. For example, in Fig. 6 where the 2.3 wt% MoO_3 on titania-coated silica after HDN reaction is imaged, one sees that all the protuberances of titania have been covered with single layers of MoS_2. The loading of Mo on the titania corresponds to about 13.7 Mo/nm^2 assuming once again that the titania surface area is equal to 7 m^2/g. The TEM images reveal that all of the protuberances are covered, so we expect that the MoS_2 loading on titania to be close to that of a monolayer of MoS_2, which is indeed the case. No stacking of the MoS_2 or multiple layers are seen in this sample. Another significant feature is the curvature of the

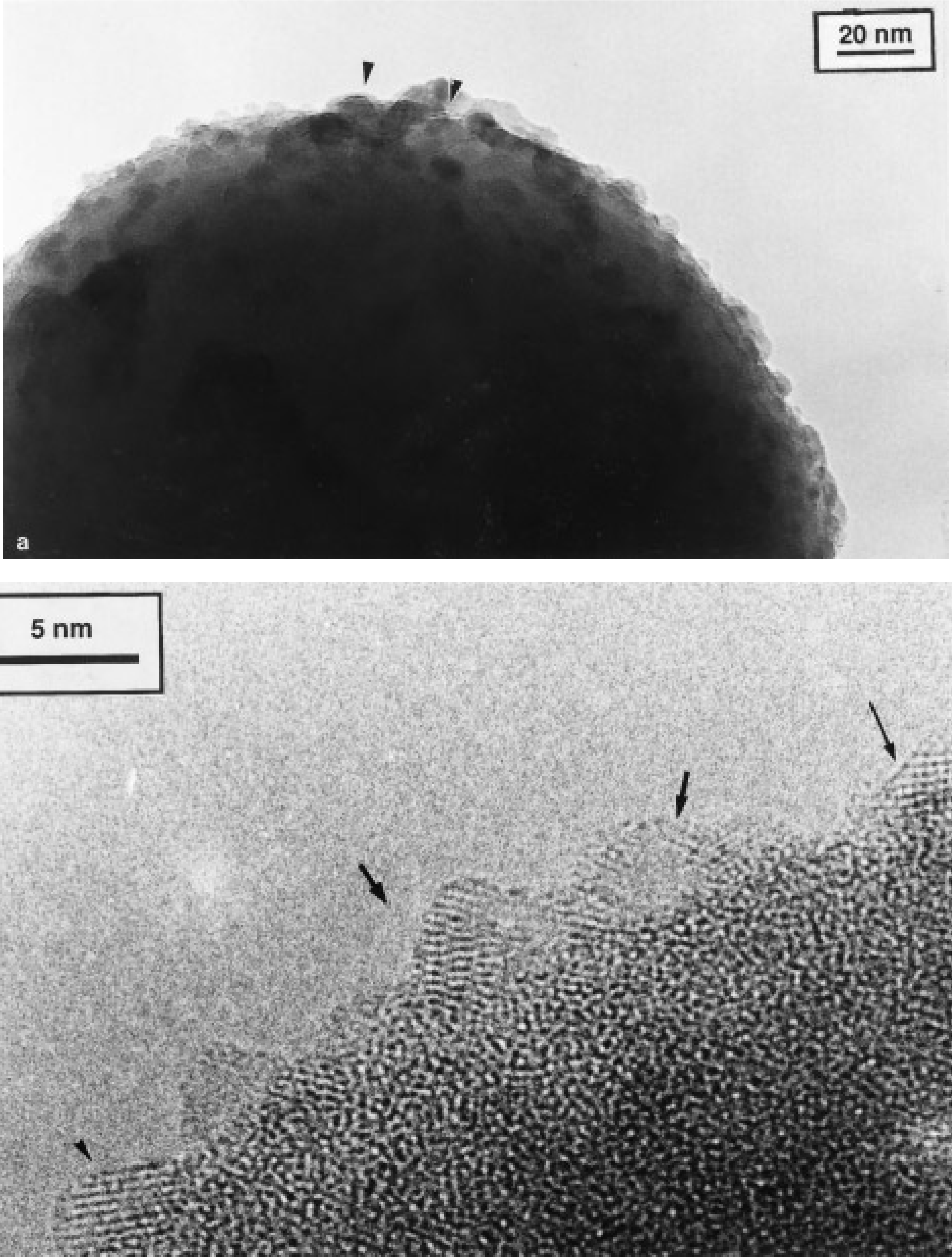

FIG. 4. Micrograph of 0.5 wt% MoO_3 on titania-coated silica after the catalyst was sulfided in 10% H_2S/H_2 at 773 K. (a) Low magnification view with the arrows showing isolated dark lines that represent the basal plane of MoS_2 on the support. (b) High magnification view showing that the TiO_2 surfaces (arrowed) which are bare. The crystalline TiO_2 exhibits lattice fringes that help distinguish it from the silica support.

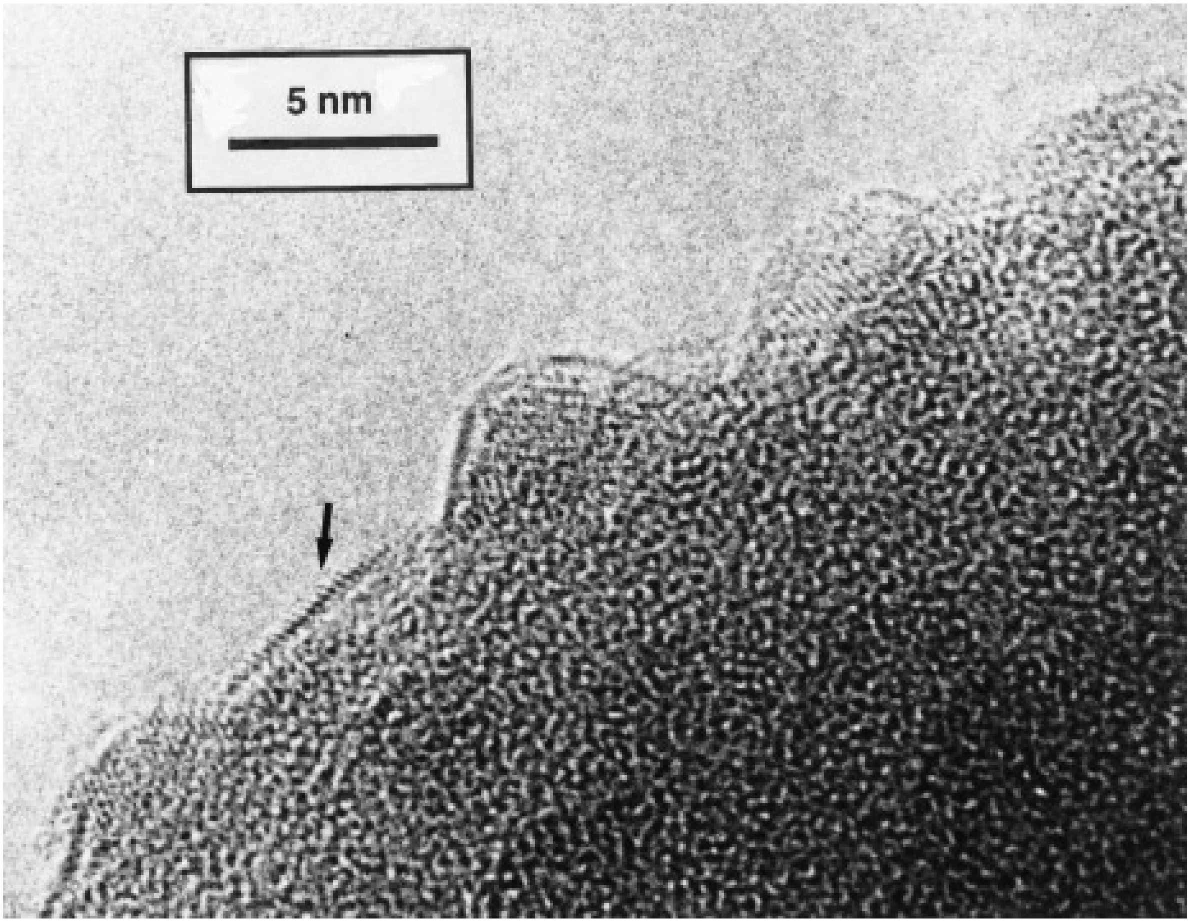

FIG. 5. High magnification view of 1.3 wt% MoO_3 on titania coated silica after the catalyst was sulfided in 10% H_2S/H_2 at 773 K. The arrow shows a flat MoS_2 segment on the silica surface. Some of the TiO_2 surface is bare.

MoS_2 layers. The MoS_2 layers form continuous curved sheets, rather than breaking up into short, straight segments. Several of these micrographs show additional structure within the dark lines that represent single layers of MoS_2. This fine structure is indicated by the arrow in Fig. 6 and consists of parallel dark lines spaced approximately 2.7 Å apart. This distance is consistent with the 2.74 Å lattice spacing for the (100) planes of MoS_2. This fine structure represents the S–Mo–S building block of the basal planes of MoS_2. In Fig. 5 the arrow indicates a flat region of MoS_2 on the silica surface. On the flat MoS_2, the fine structure shows dark lines that are parallel to each other. In contrast, the curved sheets of MoS_2 in Fig. 6 exhibit fine structure where the dark lines appear to fan out, being locally perpendicular to the titania support.

The activity of all of these catalysts for pyridine HDN was measured in a flow reactor and the results are shown in Table 2. Reactions were carried out between 633 and 673 K, and the typical product distribution consisted of 70 mole% pentane, small amounts of cyclopentane, and the remainder being hydrogenolysis products ranging from C_1–C_4. The catalyst activity for consumption of pyridine was also normalized to the amount of Mo and to the number of edge sites as determined from oxygen chemisorption data and the results are listed in Table 2. From this table, it is evident that the catalysts supported on titania/silica are more active than those supported on titania both on a mass basis and also on a per atom Mo basis. Based on the moles of oxygen chemisorbed, the MoS_2 on titania/silica samples are almost 13 to 50 times more active. The activation energies range from 23–25 kcal/mole and are comparable on both supports. The variation of specific activity (i.e., activity normalized with the chemisorption measurements) with loading is shown in Fig. 7. The Mo/TiO_2 catalysts show a decrease in activity with increasing loading, which is similar to that seen in the work of Pratt *et al.* (5). On the other hand, the Mo/titania/silica catalysts do not exhibit a marked decrease in activity with loading, and their activities are consistently an order of magnitude greater than those on the bulk titania supports. The MoS_2/titania/silica samples cover a range of surface coverages, from a fraction of a monolayer (on the 0.54

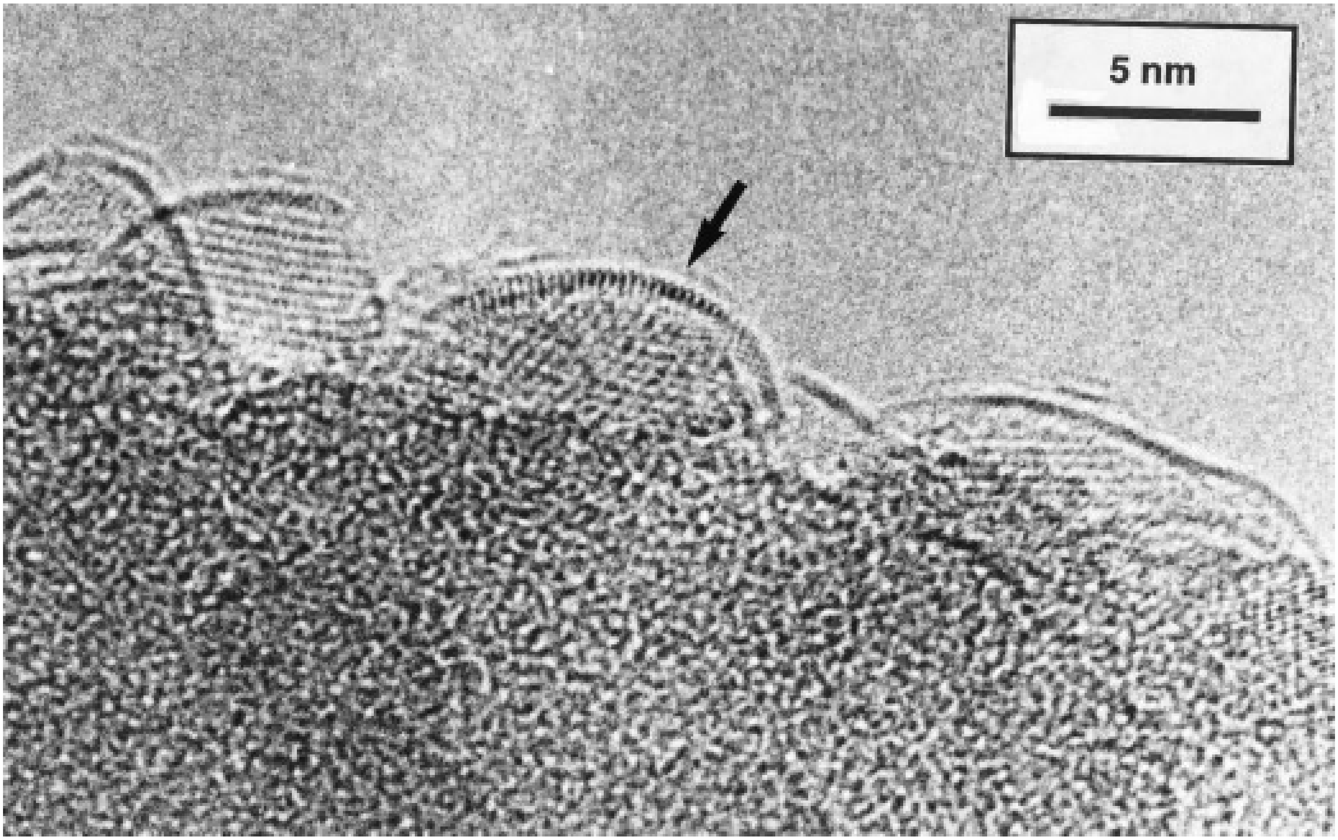

FIG. 6. High magnification view of 2.3 wt% MoO_3 on titania coated silica after the catalyst was sulfided in 10% H_2S/H_2 at 773 K. The coverage of MoS_2 exceeds that of a monolayer and all of the TiO_2 protuberances are covered. The arrow shows a fan-like fine structure within the MoS_2 basal plane.

wt% sample) to nearly that of a monolayer (on the 2.3 wt% sample).

DISCUSSION

The major finding of this study is that the MoS_2 supported on titania/silica is more reactive than MoS_2 on bulk titania for the HDN of pyridine. We have also found that the dependence of reactivity on coverage is very different for these two sets of catalysts. Let us first examine the dependence of activity on the surface coverage of MoS_2 on bulk titania. Our results shown in Fig. 7 are in agreement with the findings of Pratt *et al.* (5) who found approximately a fivefold decrease in activity on increasing the coverage of MoS_2 on titania from 0.97 to 9.73 Mo/nm^2. On alumina samples, where the coverage ranged from 0.3 to 6.0 Mo/nm^2, they found first an increase in activity with coverage with a maximum at about 1.5 Mo/nm^2 and then a drop in activity with increasing coverage. The different behaviors of the alumina- and titania-supported samples were explained based on the different morphologies adopted by MoS_2, the basal plane morphology on titania and bookend morphology on alumina. In a previous work, we have presented unambiguous evidence for the basal plane morphology on both of these supports (8) which is in agreement with the results of other workers (9, 10). What then could account for the different behavior of titania and alumina supports? The major difference we find is that on titania, with increasing coverage, a larger fraction of the MoS_2 is seen to form single layers of MoS_2, whereas on alumina, at comparable coverages, one starts to see multiple layers and stacking of the MoS_2 sheets. This is also seen in recent work by Ramirez *et al.* (11). Consequently, on titania supports, we would expect to see a steeper decline in activity since single sheets of MoS_2 would have a lower ratio of edge to basal plane sites as the size of the MoS_2 islands increases.

In light of the behavior of titania which favors the formation of single sheets of MoS_2 with increasing coverage, it is indeed surprising that the activity of the MoS_2/titania/silica catalysts does not decrease significantly as monolayer coverage of the titania is approached. The unique morphology of the titania/silica support allows us to restrict the size of the MoS_2 islands. This is because MoO_3 spreads easily on titania and prefers to wet titania in a titania/silica mixed oxide. The difference in the

TABLE 2

Catalyst Reactivity for HDN of Pyridine

Catalys support	wt% MoO_3	Specific loading Mo/nm^2	O_2 uptake (m mole/g)	Activity[a] [(mole/g sec) × 10^{12}]	Activity [(mole/mole) O_2/sec × 10^7]	Activity [(mole/mole) Mo/sec × 10^7]	Activation energy
Titania-silica	0.5	3.2	3.9	32	82	6.1	25.5
Titania-silica	1.3	7.7	4.6	91	198	8.7	25.9
Titania-silica	2.3	13.7	4.6	100	217	4.8	23.1
P25 titania	2.6	2.2	33.3	21	6.3	1.01	22.6
P25 titania	4.4	3.7	37.4	17	4.5	0.41	13.6
P25 titania	4.7	3.9	41.7	36	8.6	0.58	20.8
P25 titania	6.4	5.4	61.1	45	7.4	0.54	10.7
P25 titania	10.4	8.7	54.0	23	4.3	0.22	13.9

[a] The activity was measured at 633 K and 101 kPa.

morphology of the bulk versus the dispersed titania support can be shown schematically in Fig. 8. As seen from this figure, we can expect that the ratio of edge Mo atoms to the basal plane Mo atoms will not decrease monotonically with increasing coverage, but rather approach an asymptotic value at monolayer coverage. This must be one of the factors accounting for the difference between the bulk and dispersed titania catalysts. The oxygen chemisorption results are in agreement with this model since they do not change much with increasing coverage on the dispersed titania samples, while on bulk titania the oxygen chemisorption uptake continues to increase approximately as the square root of the Mo loading.

The difference in the size of the MoS_2 islands by itself cannot account for the increased activity of the MoS_2/titania/silica sample. From Table 2, we can see that even at the lowest loading of MoS_2, the titania/silica sample

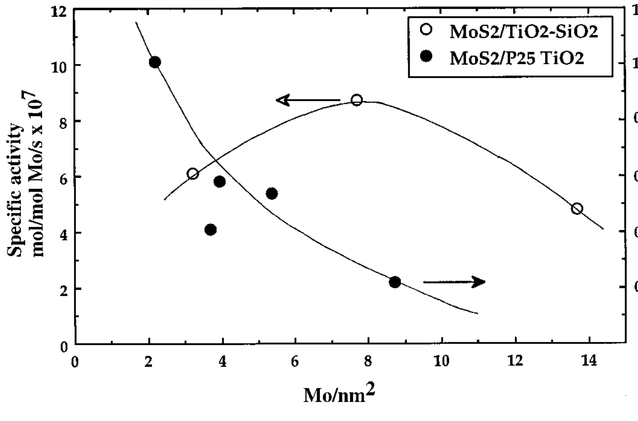

FIG. 7. Specific activity for hydrodenitrogenation with increasing Mo loading. The MoS_2 on TiO_2/SiO_2 is approximately ten times more reactive and is plotted on a different scale.

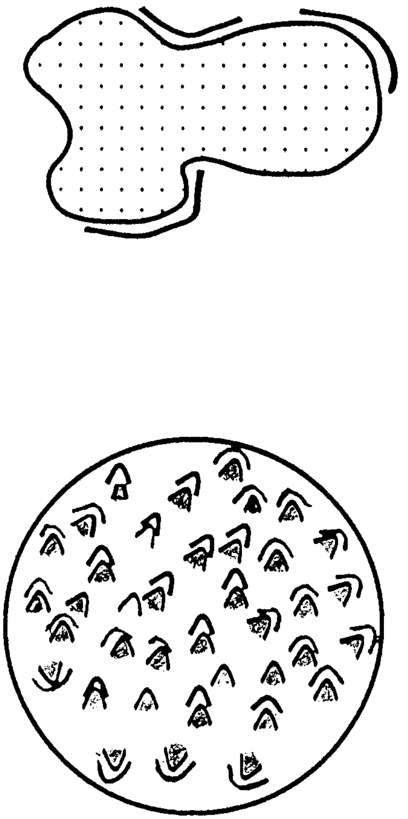

FIG. 8. Schematic illustration of the differences in the morphology of MoS_2 supported on conventional TiO_2 and our microengineered TiO_2. The black lines on the surface represent single layers of MoS_2. The figure is not to scale since the TiO_2 particles exhibiting a smooth surface are approximately 20–30 nm in diameter while the rough surface represents TiO_2 protuberances on the order of 5 nm on a 200-nm silica sphere. The smooth surface texture may facilitate the formation of large islands of MoS_2 as the coverage is increased (top). In this study we have prepared TiO_2 with a rough surface (bottom).

is more reactive than the bulk titania supported material. Therefore, we must look for some other explanation for the increased activity. Examination of the electron micrographs in Figs. 1–6 show that the MoS_2 sheets on the titania/silica are much more curved than those on bulk titania. This is a consequence of the particle size differences, approximately 28 nm for the bulk titania versus 2–5 nm for the titania–silica. These curved MoS_2 sheets would be expected to be strained and may provide access to additional sites not otherwise available from flat sheets of MoS_2. As shown in the schematic on Fig. 9, the curved MoS_2 may expose some of the Mo atoms in the basal plane or the strain may create S vacancies in the basal plane thus generating active sites also in the basal plane of MoS_2. Such a possibility was also suggested by Shimada *et al.* (3). When we examine images of supported MoS_2 reported in the literature, we find that the MoS_2 sheets are generally quite flat, or possess a modest radius of curvature, which is a consequence of the surface structure of the supports that are commercially used. High surface area alumina has a plate-like morphology where the surface area is obtained by creating pores due to loss of water during the transformation of boehmite to alumina. Furthermore, alumina favors formation of small islands of MoS_2 with multilayers, which tend to form on the flat regions of the support. The microengineered oxide supports synthesized in this study are unique in that they are able to facilitate formation of curved MoS_2 sheets with a radius of curvature ranging from 2–5 nm, not otherwise possible on commercially available catalyst supports. We suggest that the curvature of these sheets may be responsible, in part, for the high activity of the MoS_2/titania/silica catalyst.

CONCLUSIONS

A microroughened titania has been prepared that consists of nanometer-sized protuberances of titania on a silica support. These titania protuberances have been used as a support for MoS_2 hydrotreating catalysts, using pyridine hydrodenitrogenation as a test reaction. The reactivity of this microroughened catalyst for HDN is an order of magnitude greater than that of MoS_2 supported on commercial fumed titania. As the catalyst loading approaches that of monolayer coverage by MoS_2, the microroughened catalyst does not show the precipitous fall off in activity that is seen on the conventional titania support when monolayer coverages are approached. This behavior is attributed to the finite size of titania protuberances which constrain the size of the MoS_2 islands on the TiO_2/SiO_2 support. Since the MoS_2 conforms to the shape of the nanometer-sized titania protuberances, we are able to stabilize curved MoS_2 sheets having a radius of curvature ranging from 2 to 5 nm, not possible on conventional catalyst supports. Conventional TiO_2 powders typically contain larger primary particles, which cannot provide the high degree of curvature achieved on our microengineered TiO_2/SiO_2 support. We suspect that curved MoS_2 domains could result in internal lattice strain leading to vacancies and defects that could enhance the activity of basal plane Mo atoms for hydrotreating reactions.

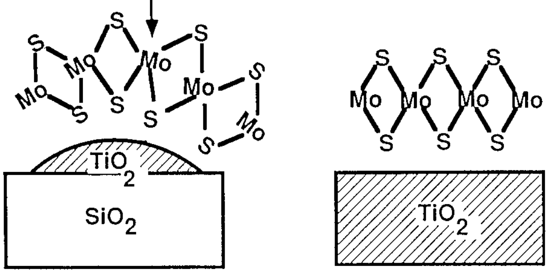

FIG. 9. Possible effect of surface curvature on the structure of supported MoS_2. The arrow indicates how a small radius of curvature may allow better access to Mo atoms in the basal plane. The strain may also create S vacancies in the basal plane.

ACKNOWLEDGMENTS

Financial support by NSF Grant CTS 89-12366 is gratefully acknowledged (A.D.). Transmission electron microscopy was performed at the electron microbeam analysis facility within the Department of Geology at the University of New Mexico. High resolution TEM was performed at the High Temperature Materials Laboratory, Oak Ridge National Lab, supported by the Under Secretary for Conservation and Renewable Energy, Department of Energy. A.D. acknowledges support via an HTML faculty fellowship. L.T.T. and J.R.B. acknowledge financial support from the National Science Foundation Presidential Young Investigator Program (CTS-9158527) and the Shell Oil Company. Pacific Northwest Laboratory is a multi-program national laboratory operated for the U.S. Dept. of Energy by Battelle Memorial Institute under Contract DE-ACO6-76RLO1830.

REFERENCES

1. Luck, F., *Bull. Soc. Chim. Belg.* **100,** 11 (1991).
2. Ramirez, J., Fuentes, S., Diaz, M., Vrinat, M., Breysse, M., and Lacroix, M., *Appl. Catal.* **52,** 211 (1989).
3. Shimada, H., Sato, T., Yoshimura, Y. Haraishi, J., and Nishijma, A., *J. Catal.* **110,** 275 (1988).
4. Ng, K. Y. S., and Gulari, E., *J. Catal.* **95,** 33 (1985).
5. Pratt, K. C., Sanders, V. J., and Christov, V., *J. Catal.* **124,** 416 (1990).
6. Chianelli, R. R., and Daage, M., *in* "Strcture-Activity and Selectivity Relationships in Heterogeneous Catalysis" (R. K. Grasseli and A. W. Sleight, Eds.), p. 137. Elsevier, Amsterdam, 1991.
7. Datye, A. K., and Smith, D. J., *Catal. Rev. Sci. Eng.* **34**(1&2), 129 (1992).
8. Srinivasan, S., Datye, A. K., and Peden, C. H. F., *J. Catal.* **137,** 513 (1992).
9. Delannay, F., *Appl. Catal.* **16,** 135 (1985).

10. Payen, E., Hubaut, R., Kasztelan, Poulet, O., and Grimblot, J., *J. Catal.* **147,** 123 (1994).
11. Ramirez, J., Ruiz-Ramirez, L., Cedeno, L., Harle, V., Vrinat, M., and Breysse, M., *Appl. Catal. A* **93,** 163 (1993).
12. Leyrer, J., Mey, D., and Knozinger, H., *J. Catal.* **124,** 349 (1990).
13. Stöber, W., Fink, A., and Bohn, E., *J. Colloid Interface Sci.* **26,** 62 (1968).
14. Srinivasan, S., Datye, A. K., Peden, Smith, M. H. S., Wachs, I. E., Deo, G., Jehang, J. M., Turek, A., and Peden, C. H. F., *J. Catal.* **131,** 260 (1991).
15. Srinivasan, S., Datye, A. K., Peden, C. H. F., and Smith, M. H. S., *J. Catal.* **145,** 565 (1994).
16. Muralidhar, G., Concha, E., Bartholomew, G. L., and Bartholomew, C. H., *J. Catal.* **89,** 274 (1984).
17. Concha, B. E., and Bartholomew, C. H., *J. Catal.* **79,** 327 (1983).
18. Zmierczak, W., Qader, Q., and Massoth, F. E., *J. Catal.* **106,** 65 (1987).